Title	Andreev and single-particle tunneling spectra of underdoped cuprate superconductors
Author(s)	Yang, KY; Huang, K; Chen, WQ; Rice, TM; Zhang, FC
Citation	Physical Review Letters, 2010, v. 105 n. 16
Issued Date	2010
URL	http://hdl.handle.net/10722/142462
Rights	Physical Review Letters. Copyright © American Physical Society.

Andreev and Single-Particle Tunneling Spectra of Underdoped Cuprate Superconductors

Kai-Yu Yang,[1,2] Kun Huang,[2] Wei-Qiang Chen,[2] T. M. Rice,[1,2,3] and Fu-Chun Zhang[2]

[1]*Institut fr Theoretische Physik, ETH Zrich, CH-8093 Zrich, Switzerland*

[2]*Center for Theoretical and Computational Physics and Department of Physics, The University of Hong Kong, Hong Kong SAR, China*

[3]*Condensed Matter Physics and Materials Science Department, Brookhaven National Laboratory, Upton, New York 11973, USA*

(Received 29 May 2010; revised manuscript received 27 July 2010; published 12 October 2010)

We study tunneling spectroscopy between a normal metal and an underdoped cuprate superconductor modeled by a phenomenological theory in which the pseudogap is a precursor to the undoped Mott insulator. In the low barrier tunneling limit, the spectra are enhanced by Andreev reflection only within a voltage region of the small superconducting energy gap. In the high barrier tunneling limit, the spectra show a large energy pseudogap associated with single particle tunneling. Our theory semiquantitatively describes the two gap behavior observed in tunneling experiments.

DOI: 10.1103/PhysRevLett.105.167004 PACS numbers: 74.72.−h, 74.20.Mn, 74.45.+c

It has long been argued that the highly anomalous pseudogap phase of underdoped (UD) cuprates holds the key to the physics of high T_c superconductors [1–4]. A variety of models have been proposed to describe this phase. At present a consensus is lacking and the merits of the different models are being vigorously debated. Some models propose the partial truncation of the Fermi surface (FS) in the pseudogap phase is due to the presence of a long range order, which breaks translational symmetry. However, in the absence of experimental evidence [5], models without this property have gained traction. These in turn can be divided into two classes. One emphasizes the reduction of the superconducting (SC) T_c by strong phase fluctuations due to the reduced superfluid density in UD cuprates. This allows the larger SC energy gaps, which in the d-wave form are maximal in the antinodal directions on the FS, to remain finite at temperatures $T > T_c$ due to preformed Cooper pairs but without off-diagonal long range order [6]. Nernst effect and diamagnetism experiments confirm the presence of SC fluctuations in an extended temperature range above T_c in the UD region of the phase diagram but the range ends substantially below the temperature scale of the onset of pseudogap behavior [7,8]. Alternative models interpret the anomalous properties of the pseudogap phase as precursor to the Mott insulator at zero doping [1], and describe the SC gap as a much lower energy scale.

Andreev tunneling has been proposed as a tool to distinguish between SC pairing fluctuations and precursor insulating in the pseudogap phase in an early paper by Deutscher [9]. In the Andreev tunneling process, an electron tunnels from a metal into a superconductor in the form of a Cooper pair and a reflected hole [10,11], which unambiguously measures the SC gap. It was pointed out that the voltage (or energy) scale in Andreev tunneling experiments on UD cuprates in the pseudogap phase [12] was substantially below that observed in the single particle tunneling experiments. The two voltage scales, however, were the same in the overdoped (OD) region. This led Deutscher to conclude in his review article that ''the balance was tilted somewhat against the preformed pairs scenario'' [13]. The opposite conclusion, namely, that the higher pseudogap energy scale reflects the pairing strength while a second lower scale, the SC condensation energy, was argued for in a later review by Hufner and co-workers which examined many experimental results using different techniques [14]. To make progress in this debate one needs to move beyond qualitative arguments about individual experiments and on to more explicit models which can be used to consistently analyze a whole range of experiments.

In this Letter, we study tunneling spectroscopy between a normal metal and UD SC cuprates, where the UD state is modeled by a phenomenological theory of Yang, Rice, and Zhang (YRZ) [15], which has been successfully applied to explain many experiments. In the low barrier or transparent tunneling limit, Andreev reflection provides an additional conducting channel. We find that the tunneling conductivity is enhanced only within a voltage region of the small SC gap. In the high barrier tunneling limit, the Andreev process is diminished. Tunneling is dominated by the single particle process, and the calculated spectroscopy shows a large pseudogap. Our theory is in good agreement with the experiments, and provides a semiquantitative description of the two gap scenario.

In the YRZ model, a single particle propagator in 2D was proposed for the pseudogap phase [15]. The model was inspired by an analysis by Konik, Rice, and Tsvelik [16] of a 2D array of lightly doped two-leg Hubbard ladders, and influenced by the functional renormalization group results at weak to moderate interaction strength [17] and by analyses of Anderson's resonant valence bond (RVB) proposal [18–20]. In this theory, the single particle

gap at the antinodes is controlled by the RVB gap which truncates the full FS into four pockets centered on the nodal directions. Such hole pockets finally evolve into large FS in OD with a vanishing RVB gap. Typical FS of the model in UD and OD are shown in Fig. 1(a). The d-wave SC energy gap opens up primarily on the Fermi pockets. The ansatz of the pseudogap as an insulating antinodal gap as proposed in the YRZ model is supported by recent numerical calculations on the 2D Hubbard model using cluster dynamical mean field theory [21].

This phenomenological propagator gives a consistent description [15] of angle resolved photoemission spectroscopy (ARPES) experiments which followed the evolution of the FS from four disconnected Fermi nodal arcs in UD to the full FS in OD cuprates [22]. It also explains a range of other spectroscopic measurements [23], e.g., the particle-hole asymmetry observed in ARPES [24], angle integrated photoemission electron spectroscopy experiments measuring the doping, x, dependence of the density of states (DOS) [25] and scanning tunneling microscopy (STM) measurements of the coherent Bogoliubov quasiparticle dispersion at low temperatures [26]. The YRZ form was also used by Carbotte, Nicol, and co-workers to successfully describe the T and x dependence of a wide range of properties in the pseudogap phase including specific heat [27], optical conductivity [28], London penetration depth [29], and symmetry-dependent Raman scattering spectra [30]. The latter was also analyzed in a similar way by Valenzuela and Bascones [31].

In the YRZ model [15], the incoherent part of the single particle Green's function contributes a smooth spectral background with a tiny real component at low energies, and the coherent part reads

$$G^0(\boldsymbol{k}, \omega) = g_t/[\omega - \epsilon_{\boldsymbol{k}} - \Sigma^0(\boldsymbol{k}, \omega)] \tag{1}$$

where $g_t = 2x/(1+x)$ is a renormalization factor [19,20]. x is the doping concentration. We use the result from

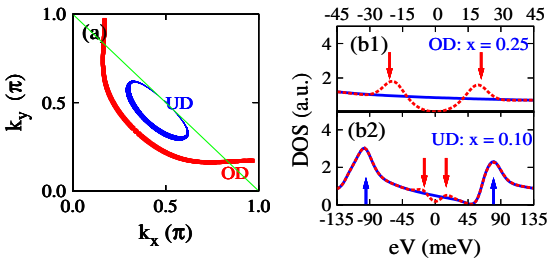

FIG. 1 (color online). Panel (a) Fermi surface in the YRZ model: Pocket (blue) for UD at doping $x = 0.1$ and (red) curve for OD at $x = 0.25$. Only a quarter of Brillouin zone is shown. The width on the pocket represents the spectral weight of quasiparticle. Thin (green) line indicates the antiferromagnetic reduced Brillouin zone. Panel (b) DOS in the model for OD (b1) and for UD (b2). Curves (blue and red) for normal (SC) state. Arrows (red) indicate SC gap, and arrows (blue) in (b2) the RVB gap at antinodes. The enhanced peak at -90 meV coincides with the van Hove singularity.

the renormalized mean field theory for the RVB state as the "bare" dispersion $\epsilon_{\boldsymbol{k}}$ [32]. The self-energy Σ^0 is zero at OD ($x > x_c = 0.2$). At UD ($x < x_c$), $\Sigma^0(\boldsymbol{k}, \omega) = [\Delta_{\boldsymbol{k}}^{\mathrm{RVB}}]^2/(\omega + \epsilon_{\boldsymbol{k}}^0)$ with $\epsilon_{\boldsymbol{k}}^0 = -2t(\cos k_x + \cos k_y)$ [32], and $\Delta_{\boldsymbol{k}}^{\mathrm{RVB}} = \Delta_0(1 - x/x_c)(\cos k_x - \cos k_y)$, with $\Delta_0 = 0.3$. All energies are in units of $t_0 (= 0.3$ eV). Note that $\epsilon_{\mathbf{k}}^0 = 0$ at the antiferromagnetic reduced Brillouin zone boundary, where the umklapp scattering is strongest [17]. Equation (1) predicts four Fermi pockets in the pseudogap phase as shown in Fig. 1(a), consistent with the recent laser ARPES data [33].

We consider a d-wave SC gap function, $\Delta_{\boldsymbol{k}}^{\mathrm{sc}} = \Delta_0^{\mathrm{sc}}(\cos k_x - \cos k_y)$ for the states around the FS within a small energy shell, $\pm\Lambda$. Several previous works proposed a similar SC pairing form for the YRZ model [15,23,29]. We choose $\Delta_0^{\mathrm{sc}} = 0.08$ for UD ($x = 0.1$), and $\Delta_0^{\mathrm{sc}} = 0.04$ for OD ($x = 0.25$). These gap parameters lead to the SC gap Δ_s (maximum $|\,\Delta_{\boldsymbol{k}}^{\mathrm{sc}}\,|$ on the FS) comparable to those observed in the Andreev reflection (~ 15 and 21 meV, respectively) [12], and to those reported in recent STM data [26]. The Green's functions for the SC state in UD and OD are,

$$\begin{aligned} G_{\mathrm{UD}}^{\mathrm{sc}}(\boldsymbol{k}, \omega) &= g_t \sum_{i=1,2} Z_{\boldsymbol{k},i} \frac{\omega + E_{\boldsymbol{k},i}\tau_z - \Delta_{\boldsymbol{k},i}^{\mathrm{sc}}\tau_x}{\omega^2 - E_{\boldsymbol{k},i}^2 - (\Delta_{\boldsymbol{k},i}^{\mathrm{sc}})^2}, \\ G_{\mathrm{OD}}^{\mathrm{sc}}(\boldsymbol{k}, \omega) &= g_t \frac{\omega + \epsilon_{\boldsymbol{k}}\tau_z - \Delta_{\boldsymbol{k}}^{\mathrm{sc}}\tau_x}{\omega^2 - \epsilon_{\boldsymbol{k}}^2 - (\Delta_{\boldsymbol{k}}^{\mathrm{sc}})^2}, \end{aligned} \tag{2}$$

where $\tau_{x/y/z}$ are the Pauli matrices, and $i = 1, 2$ denotes the lower and higher energy quasiparticle bands given by Eq. (1) for the UD region with spectral weight $g_t Z_{\boldsymbol{k},i} = g_t(1 \pm \xi_{\boldsymbol{k}}^+/E_{\boldsymbol{k}}^0)/2$ and dispersion $E_{\boldsymbol{k},i} = \xi_{\boldsymbol{k}}^- \pm E_{\boldsymbol{k}}^0$, where $\xi_{\boldsymbol{k}}^{\pm} = (\epsilon_{\boldsymbol{k}} \pm \epsilon_{\boldsymbol{k}}^0)/2$, and $E_{\boldsymbol{k}}^0 = \sqrt{[\xi_{\boldsymbol{k}}^+]^2 + [\Delta_{\boldsymbol{k}}^{\mathrm{RVB}}]^2}$. $G_{\mathrm{OD}}^{\mathrm{sc}}$ has a BCS form. In the UD region, the quasiparticle energy of the band $i = 2$ is well above the chemical potential, which justifies our choice $\Delta_{\boldsymbol{k},2}^{\mathrm{sc}} = 0$. In Fig. 1(b), we show DOS for the normal and SC states from Eqs. (1) and (2) of the model, at $x = 0.25$ (OD) and $x = 0.1$ (UD).

We use the Keldysh formalism to study the tunneling conductivity of a normal metal, superconducting state of cuprates (NS) junction, consisting of a normal metal lead at the left and a SC lead at the right as shown in Fig. 2. We approximate the connection area or line interface as a scattering center. The tunneling of an electron from the left (L) to the right (R) via the scattering center can be described by the hybridization Hamiltonian, $H' = \sum_{\boldsymbol{k},\alpha=L/R}(t_{\boldsymbol{k}}^{\alpha} c_{\boldsymbol{k},\alpha}^{\dagger} d + \mathrm{H.c.})$ with $c_{\boldsymbol{k},\alpha}$ and d the electron annihilation operators at lead $\alpha = L, R$ and on scattering center, respectively. We assume $t_{\boldsymbol{k}}^{\alpha} = t^{\alpha}$. In the tunneling process, k_x is conserved, and the total current is given by [34–36], with $\hbar = 1$,

$$\begin{aligned} I &= \sum_{s=\pm} es \int d\omega \frac{dk_x}{2\pi} \{T_N^{ss}(k_x, \omega)[f^L(\omega + seV) - f^R(\omega)] \\ &\quad + T_A(k_x, \omega)[f^L(\omega + seV) - f^L(\omega - seV)]\}, \end{aligned} \tag{3}$$

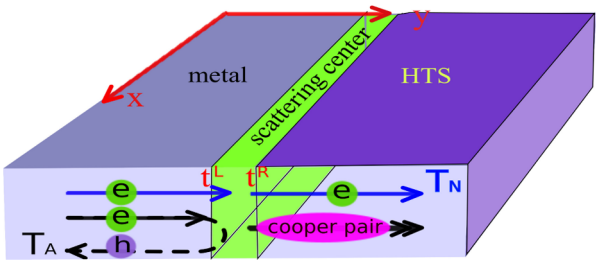

FIG. 2 (color online). Schematic plot for a metal superconductor junction. Left: normal metal; Center, scattering center, Right: Curpate superconductor. T_N and T_A represent single particle and Andreev reection tunneling.

where $f^\alpha(\omega)$ is the Fermi function at lead α. T_N^{ss}, T_A are the diagonal components of the single particle tunneling matrix T_N and the Andreev reflection coefficient, respectively. $s = +(-)$ corresponds to the electron (hole) channel. With ω dependence implied we have,

$$T_N(k_x) = G_c^a(k_x)\Gamma^L(k_x)G_c^r(k_x)\Gamma^R(k_x)$$
$$T_A(k_x) = [G_c^a(k_x)]_{12}[\Gamma^L(k_x)]_{22}[G_c^r(k_x)]_{21}[\Gamma^L(k_x)]_{11} \quad (4)$$

where $G_c^{a/r}$ refers to the advanced or retarded Green's function, $G_c(k_x) = 1/[\omega - \Sigma^L(k_x) - \Sigma^R(k_x)]$ is the Green's function in the scattering center [37]. The self energies $\Sigma^\alpha(k_x) = (t^\alpha)^2\tau_z G^\alpha(k_x)\tau_z$ and lifetime broadening $\Gamma^\alpha(k_x) = -i[\Sigma^{\alpha,a}(k_x) - \Sigma^{\alpha,r}(k_x)]$, with $G^\alpha(k_x)$ the Green's functions on the metal side or on the superconductor side given by Eqs. (1) and (2) at their edges to the scattering center. Spin rotational invariance leads to $T_N^{++}(\omega) = T_N^{--}(-\omega)$ and $T_A(\omega) = T_A(-\omega)$.

The conductance at zero temperature is given by

$$\sigma_s(eV) = \int_{-\pi}^{\pi} \frac{dk_x}{2\pi} e^2 \sum_{s=\pm} [T_N^{ss}(k_x, seV) + 2T_A(k_x, seV)]. \quad (5)$$

We consider tunneling along an antinodal direction of the CuO_2 plane, and assume a parabolic dispersion in the normal metal, $\epsilon_k^L = (k^2 - k_F^2)/2m$, setting $k_F = \pi/2$, $m = \pi/2$ in units of $1/t_0$.

We now discuss the tunneling conductance in our model and compare with experiment. We choose $t^L = \sqrt{g_t}t^R$, and a small but finite broadening δ, appearing in frequency $\omega \to \omega + i\delta$. There are two parameter regions in the tunneling. Large $t^{R/L}$ corresponds to low barrier or transparent tunneling, where Andreev reflection is substantial within the SC gap Δ_s. Simultaneously a large scattering rate $\Gamma^{R/L}$, leads to a smooth σ_n. Small $t^{R/L}$ corresponds to high barrier tunneling, where the Andreev reflection is strongly suppressed, and single particle tunneling process dominates.

The OD case is similar to a d-wave BCS superconductor. The normal state is a metal with a full FS [see the (red) curve in Fig. 1(a)] and the RVB gap vanishes. The conductance in the transparent limit is shown in Fig. 3(a). There is a marked enhancement of the conductivity σ_s over σ_n within the SC gap, which is "universal" in this limit. Note that the detailed shape of σ_s depends strongly on the parameters in the suppression of the single particle tunneling affected by the Andreev reflection. The conductance in the high barrier limit is shown in Fig. 3(b), where σ_n follows closely the normal state DOS in Fig. 1 (b1), and σ_s is similar to the single particle spectra for the d-wave SC gap, while σ_s^A is vanishingly small. σ_s in our theory agrees well with STM data [38].

For UD, there are two energy scales, a larger RVB gap or pseudogap and a smaller SC gap Δ_s. We expect two distinct energy scales in the tunneling conductance. σ_s in the transparent region is plotted in Fig. 4(a). The contribution from Andreev reflection is only substantial one within the SC gap on the FS. σ_s shows a clear peak-edge feature at the SC gap energy Δ_s. The enhancement of conductivity just outside the gap is due to the accumulation of DOS pushed outside of the gap. Our result is in good agreement with the reported Andreev tunneling experiment [12], which is reproduced here for comparison. In a single gap scenario, it is not clear that the relative contributions of Andreev and single particle tunnelings into the superconductor should change between OD and UD.

The voltage-dependent conductance in high barrier tunneling is plotted in Fig. 4(b) for UD. The Andreev reflection is substantially suppressed, so that the voltage-dependence of σ_s is similar to that of the DOS [Fig. 1(b)]. In both σ_s and DOS in the SC phase, there are two energy scales. The lower energy peak is associated with the SC gap Δ_s, and the higher energy peak with the RVB gap. The overall profile we obtained is very close to recent STM experimental data on Bi-2212 [39].

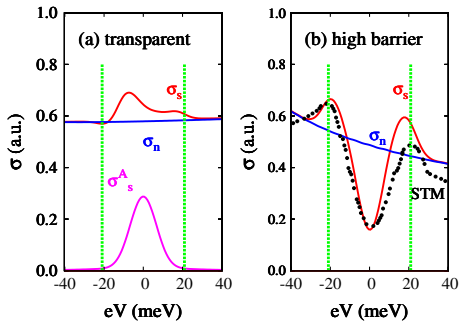

FIG. 3 (color online). Tunneling conductance at OD ($x = 0.25$). Panel (a) transparent limit $t^L = g_t^{1/2}t^R = 10$. Panel (b) high barrier limit $t^L = g_t^{1/2}t^R = 0.02$. σ_s (σ_n) for NS (normal metal, normal state of cuprates) junction, σ_s^A is the contribution to σ_s from Andreev reflection. Lines (green) indicate SC gap ($\Delta_s \sim 21$ meV). Black dots in Panel (b) are STM data of dI/dV on OD Bi2212 ($T_c = 68$ K) [38]. Lifetime broadening $\delta = 0.005$ is used in theory.

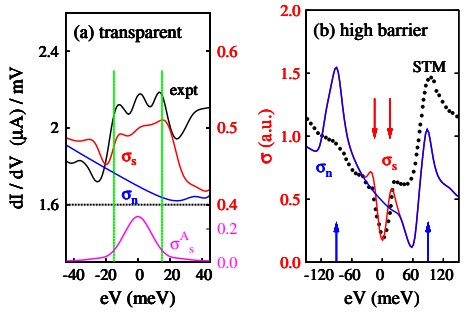

FIG. 4 (color online). Conductance at UD cuprate ($x = 0.1$) in transparent limit (a) and in high barrier tunneling limit (b). Curves (blue and red) are for σ_n (σ_s), and lower curve (magenta) in (a) is for σ_s^A (Andreev reflection contribution to σ_s). Black curves: experimental data of Andreev reflection on UD $YBa_2Cu_3O_{7-\delta}$ samples [12] [Panel (a)], and of dI/dV for UD Bi-2212 ($T_c = 45$ K) observed in STM [39] [Panel (b)]. Lines (green) in (a) and (red) arrows in (b) indicate SC gap $\Delta_s \sim 15$ meV, (blue) arrows the RVB gap (pseudogap). The parameters used are the same as in Fig. 3 for OD except the doping. Note that the negative energy RVB peak is enhanced by the van Hove singularity.

The asymmetry in the YRZ DOS comes from the Dirac quasiparticle at positive energies in the lower quasiparticle band. It is consistent with the recent angle integrated photoemission electron spectroscopy experiments [25] indicating a linear dependence of DOS at the Fermi level on the hole doping. However, it is much more pronounced than in the tunneling experiments, possibly due to the neglect of the quasiparticle lifetime broadening, which could act to smear signs of a Dirac point at finite energies above the chemical potential. The tunneling conductance in our theory does not include a spectral weight asymmetry upon injecting an electron or a hole in a strongly correlated system [40,41]. Although the long range SC order on the Fermi pockets (or arcs) induces a reduced pairing amplitude also in the antinodal regions through Cooper channel scattering, the corresponding Andreev signal is found to be strongly suppressed.

In summary, we have studied the tunneling spectroscopy of the underdoped cuprates from the viewpoint of a doped Mott insulator. Our theory semiquantitatively explains the two gap scenario at underdoping. From a broader viewpoint, our calculations support all models in which the pseudogap at underdoping is due to the partial truncation of the Fermi surface through an insulating gap in the antinodal regions, but not due to preformed Cooper pairs.

We thank M. Sigrist and Q. H. Wang for discussions. This work is partially supported by Swiss National funds and the NCCR MaNEP (K. Y. Y., T. M. R.), and Hong Kong RGC (WQC,FCZ) HKU 7056/08P, 7010/09P, and 7010/10P. T. M. R. acknowledges the support from the Center for Emergent Superconductivity, an Energy Frontier Research Center supported by the U.S. DOE, Office of Basic Energy Sciences.

[1] P. A. Lee *et al.*, Rev. Mod. Phys. **78**, 17 (2006).
[2] P. A. Lee, Rep. Prog. Phys. **71**, 012501 (2008).
[3] M. Ogata *et al.*, Rep. Prog. Phys. **71**, 036501 (2008).
[4] M. R. Norman *et al.*, Adv. Phys. **54**, 715 (2005).
[5] I. Tomeno *et al.*, Phys. Rev. B **49**, 15327 (1994).
[6] M. R. Norman *et al.*, Phys. Rev. B **76**, 174501 (2007).
[7] Y. Wang, L. Li, and N. P. Ong, Phys. Rev. B **73**, 024510 (2006).
[8] L. Li *et al.*, Phys. Rev. B **81**, 054510 (2010).
[9] G. Deutscher, Nature (London) **397**, 410 (1999).
[10] G. E. Blonder, M. Tinkham, and T. M. Klapwijk, Phys. Rev. B **25**, 4515 (1982).
[11] For a review of Andreev reflection, see S. Kashiwaya *et al.*, Rep. Prog. Phys. **63**, 1641 (2000).
[12] Y. Yagil *et al.*, Physica C (Amsterdam) **250**, 59 (1995).
[13] G. Deutscher, Rev. Mod. Phys. **77**, 109 (2005).
[14] S. Hufner *et al.*, Rep. Prog. Phys. **71**, 062501 (2008).
[15] Kai-Yu Yang, T. M. Rice, and F. C. Zhang, Phys. Rev. B **73**, 174501 (2006).
[16] R. M. Konik, T. M. Rice, and A. M. Tsvelik, Phys. Rev. Lett. **96**, 086407 (2006).
[17] C. Honerkamp *et al.*, Phys. Rev. B **63**, 035109 (2001).
[18] P. W. Anderson, Science **235**, 1196 (1987).
[19] F. C. Zhang *et al.*, Supercond. Sci. Technol. **1**, 36 (1988).
[20] P. W. Anderson *et al.*, J. Phys. Condens. Matter **16**, R755 (2004).
[21] M. Ferrero *et al.*, Phys. Rev. B **80**, 064501 (2009).
[22] A. Damascelli *et al.*, Rev. Mod. Phys. **75**, 473 (2003).
[23] Kai-Yu Yang *et al.*, Europhys. Lett. **86**, 37002 (2009).
[24] H.-B. Yang *et al.*, Nature (London) **456**, 77 (2008).
[25] M. Hashimoto *et al.*, Phys. Rev. B **79**, 140502 (2009).
[26] Y. Kohsaka *et al.*, Nature (London) **454**, 1072 (2008).
[27] J. LeBlanc, E. J. Nicol, and J. P. Carbotte, Phys. Rev. B **80**, 060505(R) (2009).
[28] E. Illes, E. J. Nicol, and J. P. Carbotte, Phys. Rev. B **79**, 100505(R) (2009).
[29] J. P. Carbotte *et al.*, Phys. Rev. B **81**, 014522 (2010).
[30] J. LeBlanc, J. P. Carbotte, and E. J. Nicol, Phys. Rev. B **81**, 064504 (2010).
[31] B. Valenzuela and E. Bascones, Phys. Rev. Lett. **98**, 227002 (2007).
[32] "Bare" dispersion from the renormalized mean field theory (see Refs. [15,19]) for the t-J model is used, $\epsilon_{\mathbf{k}} = -2t(c_x + c_y) - 4g_t t' c_x c_y - 2g_t t''(c_{2x} + c_{2y}) - \mu$ with $c_{ax/y} = \cos ak_{x/y}$ and parameters $t = (g_t + \frac{3}{8} g_s J\chi)$, $t' = -0.4$, $t'' = 0.2$, $J = 0.3$ (in units of t_0), $\chi_0 = 0.338$, $g_s = 4/(1+x)^2$.
[33] J. Meng *et al.*, Nature (London) **462**, 335 (2009).
[34] M. Yigal and N. S. Wingreen, Phys. Rev. Lett. **68**, 2512 (1992).
[35] Q. F. Sun *et al.*, Phys. Rev. B **59**, 3831 (1999).
[36] Da Wang, Y. Wan, and Q. H. Wang, Phys. Rev. Lett. **102**, 197004 (2009).
[37] In the high barrier limit, the scattering center has a constant tunneling channel at all energies.
[38] A. N. Pasupathy *et al.*, Science **320**, 196 (2008).
[39] Y. Kohsaka *et al.*, Science **315**, 1380 (2007).
[40] P. W. Anderson *et al.* J. Phys. Chem. Solids **67**, 1 (2006).
[41] M. Randeria *et al.*, Phys. Rev. Lett. **95**, 137001 (2005).